Behavior of Supercoiled DNA

T. R. Strick, J.-F. Allemand, D. Bensimon, and V. Croquette
Laboratoire de Physique Statistique de l'ENS, URA 1306 CNRS, Associé aux Universités Paris VI et VII, 75231 Paris Cedex 05, France

ABSTRACT We study DNA supercoiling in a quantitative fashion by micromanipulating single linear DNA molecules with a magnetic field gradient. By anchoring one end of the DNA to multiple sites on a magnetic bead and the other end to multiple sites on a glass surface, we were able to exert torsional control on the DNA. A rotating magnetic field was used to induce rotation of the magnetic bead, and reversibly over- and underwind the molecule. The magnetic field was also used to increase or decrease the stretching force exerted by the magnetic bead on the DNA. The molecule's degree of supercoiling could therefore be quantitatively controlled and monitored, and tethered-particle motion analysis allowed us to measure the stretching force acting on the DNA. Experimental results indicate that this is a very powerful technique for measuring forces at the picoscale. We studied the effect of stretching forces ranging from 0.01 pN to 100 pN on supercoiled DNA ($-0.1 < \sigma < 0.2$) in a variety of ionic conditions. Other effects, such as stretching-relaxing hysteresis and the braiding of two DNA molecules, are discussed.

INTRODUCTION

Vinograd first understood in 1965 (Vinograd et al., 1965) that the double-helical nature of DNA allows it to be overwound and underwound from its natural state. Today we know that DNA is topologically polymorphic. The overwound or underwound double helix can assume exotic forms known as plectonemes (like the braided structures of a tangled telephone cord) or solenoids (similar to the winding of a magnetic coil) (Marko and Siggia, 1995). These tertiary structures have an important effect on the molecule's secondary structure and eventually its function. For example, supercoiling-induced destabilization of certain DNA sequences can allow the extrusion of cruciforms (Palacek, 1991) or even the transciptional activation of eukaryotic promoters (Dunaway and Ostrander, 1993). We study the supercoiling of DNA by single-molecule techniques to better understand the relations between the physical form and biological function of DNA.

Consider, for example, the packaging of eukaryotic genomes. In human cells, the nucleus is just a few microns on a side, yet it must contain ~3 m of DNA, divided into 46 chromosomes. If these chromosomes were in the form of a random coil, they would not fit inside the nucleus. As was shown by Patterton and von Holt (1993), negative supercoiling favors DNA-histone association and the formation of nucleosomes (the first step in packaging DNA). Because the solenoidal DNA wrapping around a nucleosome core creates about two negative supercoils, it is understandable that DNA which fulfills this topological prerequisite will more easily form nucleosomes. Another essential process, DNA transcription, can both generate and be regulated by supercoiling. In vitro (Wang and Dröge, 1997) and in vivo (Wu et al., 1988) studies have shown that the processive motion of an RNA polymerase along its template creates positively supercoiled domains ahead of the transcription complex and negatively supercoiled domains behind (Dunaway and Ostrander, 1993).

DNA replication poses a similar but topologically enhanced problem. Once replication is completed, the newly synthesized molecule must be disentangled from its parent. The replication of circular DNA molecules gives rise to two linked circular molecules, but the replication of whole chromosomes leaves the cell with highly entangled chromatids. If the cell does not disentangle the freshly replicated pairs of sister chromatids, they will fragment under the pull of the mitotic spindle. Disentanglement is achieved thanks to topoisomerases (Jannink et al., 1996). Topoisomerases are the cell's tools for managing the topologies of their genomes (Wang, 1996). Type I topoisomerases act by transiently breaking one of the strands of duplex DNA, allowing the intact strand to pass through and thereby changing the number of times the two strands wrap. Type II topoisomerases transiently break both strands of duplex DNA, allowing another segment of duplex DNA to pass through. Type II topoisomerases thus have an unknotting activity, which is required to disentangle linked circles or replicated chromosomes.

Thus DNA supercoiling has been extensively studied because it links the biological activity of DNA to its tertiary structure and not just its sequence. The techniques employed have ranged from electron cryomicroscopy images of supercoiled plasmids (Boles et al., 1990; Bednar et al., 1994) to electrophoretic gel-mobility shift assays to characterize and describe supercoiled DNA topoisomers. Molecular dynamics and Monte Carlo simulations have also helped give an idea of the types of structures present in

Received for publication 11 August 1997 and in final form 9 December 1997.

Address reprint requests to T. R. Strick, Laboratoire de Physique Statistique de l'ENS, URA 1306 CNRS, associé aux universités Paris VI et VII, 24 rue Lhomond, 75231 Paris Cedex 05, France. Tel.: 33-1-44-32-34-92; Fax: 33-1-44-32-34-33; E-mail: strick@clipper.ens.fr.

0006-3495/98/04/2016/13 $2.00

supercoiled molecules (Schlick and Olson, 1992; Klenin et al., 1995; Vologodskii et al., 1992). Until recently, it was only possible to control the supercoiling of plasmid DNAs by using intercalators (such as ethidium bromide) or commercially available topoisomerases. These techniques have several disadvantages. They do not allow for real-time modification and analysis of DNA supercoiling; nor do they allow for precise, controlable, and reversible DNA supercoiling. Finally, traditional supercoiling assays are only functional on large ensembles of closed circular DNA molecules. We have established a new technique based on the tools of DNA micromanipulation that gives us the possibility of executing precise, quantitative, and reversible supercoiling of an individual linear DNA molecule in real time.

To do so, we have constructed an experimental system inspired by the experiments of Smith et al. (1992) concerning the stretching of an individual DNA molecule. By binding a single DNA molecule by one end to a treated glass surface and by the other end to a small magnetic bead, Smith et al. (1992) were able to measure the stretching force on a DNA molecule due to a combination of magnetic and hydrodynamic forces. They were then able to establish, with the help of J. Marko and E. Siggia (Bustamante et al., 1994), that the elastic behavior of torsionally relaxed DNA resembles that of a semiflexible polymer, a worm-like chain (WLC) (see below for details). The DNA flexibility is represented by its persistence length: $\xi \approx 50$ nm in physiological conditions. This is the distance over which the orientation of the chain becomes uncorrelated: the stiffer the chain, the longer its persistence length (Flory, 1969; de Gennes, 1979).

The DNA molecules used in Smith's experiment (Smith et al., 1992) were bound by a single biochemical link at their extremities. As the DNA is free to swivel about its anchors, no torsional constraints could be applied to these molecules. By using a DNA construct presenting multiple binding sites at its extremities, we have added to these experiments the possibility of exerting a torsional constraint on an unnicked molecule.

We can mechanically overwind and underwind the bound DNA by using a rotating magnetic field to induce the synchronous rotation of the magnetic bead to which the DNA is bound. DNA can thus be coiled in a continuous, controllable, and reversible fashion in real time. Furthermore, with the use of a novel technique based on the analysis of the Brownian motion of the tethered bead (Gelles et al., 1988; manuscript in preparation), we can measure the stretching force applied to a single coiled DNA molecule. In this paper we describe the behavior of individual DNA molecules subjected to stretching forces varying between 0.01 pN and 100 pN, under different ionic conditions and various degrees of supercoiling, both positive and negative. We also present results concerning the braiding of two DNA molecules around each other.

BASICS OF DNA SUPERCOILING AND STRETCHING

Initial studies of DNA supercoiling have been carried out on small circular DNA molecules (plasmids). The circularity of these DNAs is useful in that it allows one to constrain the extremities of the molecule by a kind of boundary condition. Linear DNA molecules may also be torsionally constrained, by anchoring them (at their extremities or along their length) to an immobile surface or a massive object. The anchoring of chromatin to the nuclear scaffold, for example, may generate topologically independent domains. The topology of such torsionally constrained molecules can then be described by a few simple quantities (White, 1969; Calladine and Drew, 1992). The first is the twist (Tw) of the molecule, the number of times the two strands that make up the double helix twist around each other. For unconstrained B-DNA this is known to be one turn every 10.4 bp. Overwinding increases the twist, underwinding decreases it. The second topological quantity of interest is the writhe (Wr) of the molecule. On a twisted phone cord one often notices the formation of interwound structures, called *plectonemes* (from the Greek meaning "braided string"), which appear to be a way of releasing torsional stress. In these structures the number of times the cord loops over itself is its writhing number, and a positive or negative value may be assigned to it. The writhe represents another type of wrapping—that of the molecule's axis with itself.

If one constrains the ends of the DNA molecule, then the total number of times that the two strands of the helix cross each other (either by twist or by writhe) becomes a topological invariant of the system known as the linking number, Lk. For a circular plasmid the only way to change Lk is to break a strand and modify the number of times the DNA winds. In the case of linear anchored molecules, however, rotating one end of the molecule allows one to access and modify Lk without damaging the DNA. A mathematical theorem due to White (1969) states that

$$Lk = Tw + Wr \tag{1}$$

The linking number of a torsionally relaxed (linear or circular) DNA is written as $Lk_0 = Tw_0 + Wr_0$. Tw_0 is the number of helical repeats in B-DNA. $Wr_0 = 0$, assuming that DNA has no significant spontaneous curvature with which it could form coils or loops. The relative difference in linking number between the supercoiled and relaxed forms of DNA is called the excess linking number, σ:

$$\sigma = \frac{Lk - Lk_0}{Lk_0} \tag{2}$$

The molecule is overwound when σ is positive and underwound when it is negative.

As mentioned earlier, the first experiments concerning the force versus extension characteristics of single DNA molecules were carried out on torsionally unconstrained DNA (Smith et al., 1992). A good fit over the full range of

their data was achieved (Bustamante et al., 1994) by treating the DNA as a worm-like chain. At low stretching forces such a system behaves like a random walk

$$F = \frac{3}{2}\frac{k_B T}{\xi}\frac{x}{l_0}$$

where F is the applied force, k_B is the Boltzmann constant, T is the temperature, ξ the walk's persistence length, and x/l_0 is the walk's relative extension. At high forces, the WLC's relative extension tends toward 1: $x/l_0 \approx 1 - 1/\sqrt{F}$. A useful interpolation formula, correct to within 10%, was proposed (Bustamante et al., 1994) to join these two regimes at intermediary forces:

$$\frac{F\xi}{k_B T} = \frac{1}{4}\left[\left(1 - \frac{x}{l_0}\right)^{-2} - 1\right] + \frac{x}{l_0} \qquad (3)$$

where x is the polymer's extension and l_0 its contour length. In this paper we fit the WLC model's exact numerical solution (manuscript in preparation) to the experimental data to extract the contour length l_0 and the persistence length ξ of the system being stretched. One may thus determine a crucial parameter: the number of molecules being stretched. Indeed, a two-molecule system is twice as stiff as a single-molecule system. As a consequence, the effective persistence length of a two-molecule system is half that of a single molecule (see Fig. 3 *A*). In our experiments we can thus distinguish between DNA supercoiling (one DNA molecule) and DNA braiding (two DNA molecules).

MATERIALS AND METHODS

Overview of setup

We bind 60-kb linear DNA molecules to small streptavidin-coated superparamagnetic beads in a phosphate-buffered saline solution. The bead-DNA complexes are then incubated in a phosphate buffer inside a square glass capillary tube that has been functionalized with anti-digoxigenin. DNA is thereby bound by one end to an immobile support (the capillary tube) and by the other end to a mobile support (the magnetic bead). The capillary, linked to a buffer-flow system, is placed over the objective of an inverted microscope (Fig. 1). Magnets located above the sample control the force applied to the bead and its rotation. The video data of a CCD camera are fed into a PC. From these data we extract the magnetic bead image; its x, y, and z coordinates (manuscript in preparation); and the force exerted on the bead.

DNA construction

A schematic explanation of the DNA construction can be found in Fig. 2. Fifty micrograms of phage λ-DNA (Boehringer-Mannheim, Meylan, France) are precipitated and resuspended in distilled water to eliminate any organic buffers. Two batches of this DNA are aliquoted; the first is subjected to two successive rounds of photolabeling in the presence of 25 μg of photoactivatable biotin (Pierce, Montlucon, France). Photolabeling reactions are carried out according to the Pierce protocol: DNA at a concentration of 1 μg/μl is mixed with an equal volume of photobiotin (also at a concentration of 1 μg/μl). The reaction tube is left open and placed in an ice bath, 10 cm away from a 40-W, 360-nm sunlamp for 10 min. The process is repeated, with the addition of another 25 μl of photobiotin. A second aliquot of purified DNA is subjected to the same sequence of labeling reactions, except that photoactivatable digoxigenin (Boehringer-Mannheim) is used as the labeling molecule. Both batches of labeled DNA are then precipitated in cold ethanol and resuspended in Tris-HCl (10 mM) and EDTA (1 mM) ($T_{10}E_1$). They are then digested by 10 units of restriction enzyme *Nru*1 (New England Biolabs, Montigny-le-Bretonneux, France) at 37°C in the enzyme's buffer. The cohesive left (4600 bp) and cohesive right (6700 bp) fragments are isolated on an ethidium-bromide free, 0.6% agarose gel in 1× Tris-acetate-EDTA (TAE)

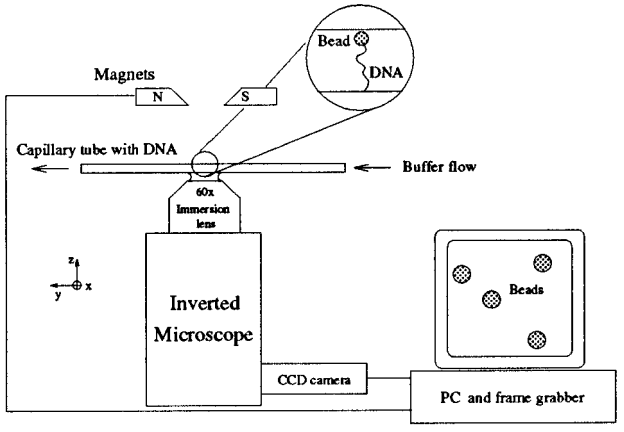

FIGURE 1 An overview of the experimental setup. The ~16-μm-long DNA molecule is bound to a glass surface (the bottom of a 1 mm × 1 mm × 50 mm capillary tube) at one end by digoxigenin/anti-digoxigenin links and at the other end to a superparamagnetic bead (3-μm diameter) by biotin/streptavidin links. The magnetic field used to pull on the bead and control its rotation is generated by Co-Sm magnets and focused by asymmetrical polar pieces with a 1.7-mm gap. This magnetic device can rotate about the optical axis, inducing synchronous rotation of the magnetic bead, and it can be lowered (raised) to increase (decrease) the stretching force. The samples are observed on a Nikon Diaphot-200 inverted microscope with a 60× immersion oil objective. Video data relating the Brownian motion of the magnetic bead is generated by a square pixel XC77CE Sony camera connected to a Cyclope frame grabber (timed on the pixel clock of the camera) installed in a 486–100-MHz PC.

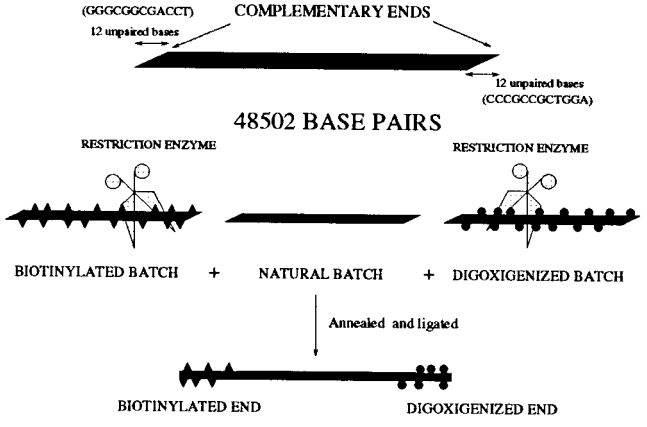

FIGURE 2 Schematic representation of the DNA construct. A segment of photochemically labeled DNA is affixed to each end of a 48.5-kb phage λ-DNA. A 5-kb fragment tagged roughly every 200–400 bp with a biotin label is annealed and ligated to the cohesive left end of the λ-DNA. A 6-kb fragment is similarly tagged with digoxigenin molecules, and then annealed and ligated to the cohesive right end of the λ-DNA. The final construct, measuring ~20 μm, is biochemically labeled over 20% of its length.

running buffer. They are then purified with the GeneCleanII system (Bio101, France), precipitated in cold ethanol and resuspended in 10 μl of $T_{10}E_1$. The cohesive-left biotin-labeled fragments are then annealed for 24 h at 37°C to intact λ-DNA molecules suspended in $T_{10}E_1$ and 10 mM $MgCl_2$, and ligated for 1 h at 37° with 5 units of T4 DNA ligase (Boehringer-Mannheim). The cohesive-right digoxigenin-labeled fragments are annealed and ligated to the reaction product in an identical manner. The final construction is thus 59.8 kb long, with biotin and digoxigenin end-labels making up 11.3 kb. Comparative experiments were also carried out on a similar pXΔ1 construct donated by F. Caron (Cluzel, 1996).

Preparation of capillary tube

Glass capillary tubes (1 mm × 1 mm × 50 mm; VitroDynamics, Mountain Lakes, NJ) are either silanized (Bensimon et al., 1994) or coated with polystyrene (Allemand et al., 1997). Five micrograms of polyclonal anti-digoxigenin (Boehringer-Mannheim) are then incubated in these tubes for at least 2 h at 37°C (or overnight at 4°C) in 100 μl of 10 mM phosphate-buffered saline (PBS). Unbound anti-digoxigenin is eliminated by rinsing with a 10 mM phosphate buffer at pH 8, supplemented with 0.1% Tween-20 and 3 mM NaN_3. The treated surface is passivated for at least 2 h at 37°C (or overnight at 4°C) with a solution consisting of 10 mM phosphate buffer at pH 8, supplemented with 0.1% Tween-20, 1 mg/ml sonicated fish sperm (FS) DNA (Boehringer-Mannheim), and 3 mM NaN_3. The tube is then rinsed and attached to a buffer flow system consisting of small plexiglass wells.

Other experiments were performed in a hermetic environment. To this end, glass coverslips (d = 18 mm) are silanized (Bensimon et al., 1994). A well is then formed by gluing to these silanized coverslips a small PVC ring (d = 12 mm, 2 mm high). The wells were coated with anti-digoxigenin and passivated as previously described, and 200 μl of the DNA-bead assembly is loaded onto the surface. After a delicate rinse of unbound beads, the wells are supplemented with a salt solution to obtain the final desired ionic concentration. The wells are sealed on top with a round glass coverslip glued with nail polish.

Construct assembly

The advantage of the DNA construction that is labeled over 20% of its length is that it allows for torsionally constraining the molecule's extremities when it is bound to an appropriate substrate. As a bonus, the binding efficiency of the DNA to the treated glass surface and the magnetic bead is greatly enhanced by this multiple labeling. Approximately 10^7 DNA molecules are incubated in 10 μl PBS with 8 μl of streptavidin-coated superparamagnetic beads (Dynal M280 or M450), previously washed three times in PBS. The reaction is stopped after 5 min by the addition of 90 μl of standard solution (10 mM PB pH 8, 0.1% Tween, 0.1 mg/ml FS DNA, and 3 mM NaN_3, referred to hereafter as 10 mM PB or 10 mM phosphate buffer). Twenty microliters of that mix is further diluted in 80 μl of standard solution and injected into the capillary tube. As the beads sediment to the capillary's "floor," they bring the DNA molecules in contact with the anti-digoxigenin-coated surface. The bead-DNA constructs are then left to incubate for at least 2 h before studies begin. We can increase the number of supercoilable (unnicked) molecules by performing a ligation reaction with T4 DNA ligase, either before or after the bead-DNA complex is injected into the capillary.

Magnetic control of DNA torsion and extension

The magnetic field we use to control the superparamagnetic bead is generated by Co-Sm magnets. It is focused by soft iron pole pieces with a 1.7-mm gap. The magnets and pole pieces are mounted on a rotating disk. Rotation of this disk is controlled by a stepper motor through an RS232 port. When the disk is at rest, the magnetic field lines are parallel to the x axis of the experiment (perpendicular to the axis of the capillary tube), and the gradient is along the z axis. The orientation of the bead is fully coupled to that of the magnets, and rotation of the bead is observed to be synchronous with rotation of the magnets (manuscript in preparation). This allows us to control the rotation of the bead and thus the coiling of the molecule bound to the bead. The rotating disk itself is attached to a translation stage that allows for vertical displacements of the disk-magnet assembly. A second motor controls these displacements via a stepper motor, allowing us to control the height of the magnets relative to the sample. We therefore use these magnets to control both the magnetic force acting on the bead (and thus on the molecule) and the degree of supercoiling of the DNA construction.

Optical videomicroscopy

The samples are observed on a Nikon Diaphot-200 inverted microscope with a 60× oil-immersion objective. Video images (25 images/s) are obtained with a square pixel XC77CE Sony camera feeding into a Cyclope frame grabber. The frame grabber is timed off the pixel clock of the camera. A 486 PC serves as the host for the frame grabber. The spatial scale of the images in the horizontal imaging plane was calibrated by using a Nikon grating. Vertical displacements are measured (and calibrated versus the microscope vertical vernier) with a small laser diode attached to the objective turret and aimed at a photodetector fixed on the microscope.

Image analysis and force measurements

The force measurement technique we use is described in detail in a forthcoming paper. The video data obtained from the apparatus described above are treated in real time to extract the Brownian motion of the tethered magnetic bead. A tracking algorithm, coded by fast Fourier transform-based correlation techniques, determines the relative displacements of the center position of the magnetic bead to a resolution of ~10 nm. This allows us to obtain Brownian motion plots representing the 3D position $\{x(t), y(t), z(t)\}$ of the bead over time.

The DNA-tethered bead, pulled a distance $l = \langle z \rangle$ by a magnetic force F, is completely equivalent to a damped pendulum. Its longitudinal ($\delta z^2 = \langle z^2 \rangle - \langle z \rangle^2$) and transverse δx^2 fluctuations are characterized by effective rigidities, $k_\parallel = \partial_z F$ and $k_\perp = F/l$. By the equipartition theorem they satisfy (Reif, 1965)

$$\delta z^2 = \frac{k_B T}{k_\parallel} = \frac{k_B T}{\partial_z F} \tag{4}$$

$$\delta x^2 = \frac{k_B T}{k_\perp} = \frac{k_B T l}{F} \tag{5}$$

where k_B and T are, respectively, the Boltzmann constant and the temperature ($k_B T = 4 \times 10^{-21}$ J = 0.6 kcal/mol). Thus, from the bead's Brownian fluctuations (δx^2, δy^2), one can extract the force F pulling on the bead (and on the tethering molecule), and from δz^2 one obtains its first derivative, $\partial_z F$. Our experimental results show that this technique allows for in situ force measurements over a large range of forces, from ~10 fN, where $\delta x \approx$ 1 μm, to a 100 pN, where $\delta x \approx$ 10 nm (Fig. 3 *B*).

RESULTS

In our experiments we control the degree of supercoiling (σ) of the molecule and the stretching force (F) applied to it. We then measure the resulting extension (l) of the DNA and normalize it by the full length l_o. Hence we usually measure force versus extension curves at a constant degree of supercoiling, or extension versus supercoiling curves at constant force. Experiments were carried out in various ionic conditions at pH 8.

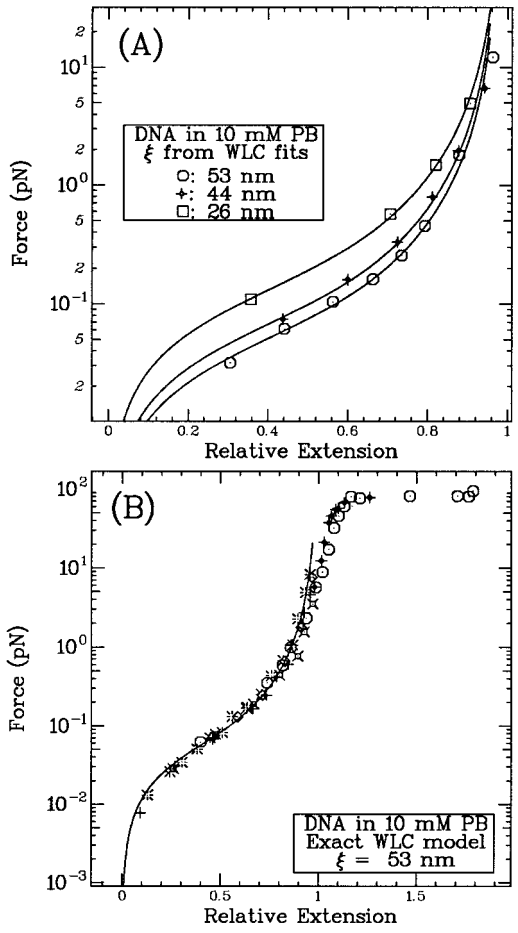

FIGURE 3 Force versus extension curves for various torsionally relaxed λ-DNA molecules in 10 mM PB. (*A*) These curves are well described (see *continuous curves*) by a worm-like chain (WLC) model with a persistence length of ~53 nm (for a single DNA molecule). With two λ-DNAs the rigidity is doubled, resulting in a halving of the effective persistence length (26 nm). We also observed systems characterized by a rigidity equivalent to a WLC with a 44-nm persistence length. This can be accounted for by the anchoring of two different DNA molecules on the bead: a regular λ-DNA and a dimer consisting of two annealed λ-DNAs. (*B*) A compendium of measurements on beads bound by a single DNA molecule over a large range of forces: 0.005 pN < F < 100 pN. The plateau at $F \approx 70$ pN (where the DNA extension increases from 1.1 to 1.8 times its crystallographic length; Cluzel et al., 1996; Smith et al., 1996) was measured by steadily increasing the force applied to a nicked molecule. These results demonstrate the wide range and precision of our measurement technique.

Torsionally relaxed DNA

We begin by presenting force versus extension curves obtained on torsionally relaxed DNA molecules ($\sigma = 0$) in 10 mM PB (Fig. 3). These results show that our measurement technique allows us to study a wide range of forces with high resolution and to distinguish a bead tethered by a single DNA molecule from one bound by two or more (Fig. 3 *A*). At low stretching forces ($0.02 < F < 2$ pN) a DNA molecule behaves like an ideal polymer chain. It can be described to a very good approximation by an ideal worm-like chain (WLC) model (Bustamante et al., 1994); fitting this model to our data allows us to extract the DNA persistence length $\xi \approx 53$ nm (consistent with previous experimental results; Smith et al., 1992; Bustamante et al., 1994) and the molecule's crystallographic length l_0. Because the labeled ends may not bind on their full length to the surfaces, l_0 varies between 16.2 μm and ~18 μm. Beads tethered to the surface by two DNA molecules yield force-extension curves characterized by a persistence length $\xi \approx$ 26 nm (half that of a single DNA molecule). We were also able to distinguish cases in which a bead was bound to the surface by two molecules: the first was a regular λ-DNA, and the second was a λ-DNA dimer. Such a system turns out to behave as if bound by a worm-like chain with a persistence length $\xi = 44$ nm. At low ionic strength (1 mM PB), ξ was seen to increase to ~75 nm; these various results are consistent with previous measurements of the salt dependence of the DNA persistence length (Smith et al., 1992).

We were also able to reproduce the high-force ($F > 10$ pN) DNA overstretching experiments first reported by Cluzel et al. (1996) and Smith et al. (1996) (Fig. 3 *B*). In these experiments, we replaced the 2.8-μm-diameter superparamagnetic beads with 4.5-μm-diameter beads. This allows us to achieve stretching forces as high as 100 pN. At a stretching force of ~70 pN, we observe the reported abrupt transition (Cluzel et al., 1996; Smith et al., 1996) in the DNA's extension as it passes from 1.1 to 1.8 times l_0. These results demonstrate the wide range of forces that can be measured with the present force measurement technique.

Supercoiled DNA

Supercoiled DNA in moderate ionic conditions (10 mM PB)

Fig. 4 shows the λ-DNA's extension as a function of supercoiling at three different forces. At a low force ($F = 0.2$ pN) the elastic behavior of DNA is symmetrical under positive or negative supercoiling. Like a phone cord, the molecule continuously "contracts" as each added turn allows it to form plectonemes and "shorten." At an intermediate force ($F = 1$ pN), the chiral nature of the molecule is evident. The extension of the molecule does not change as it is underwound, whereas it continues to contract when overwound. Finally at high forces (here $F = 8$ pN), the DNA's extension depends only slightly on the degree of supercoiling and is similar to that expected from a torsionless worm-like chain.

These three regimes are also evident in the force versus extension plots at fixed σ (Fig. 5):

- At low forces ($F < 0.5$ pN) under- and overwound DNA molecules at the same value of $|\sigma|$ have essentially the same extension at a given force. Their rigidity, the force required to stretch the molecule to a given length, increases with $|\sigma|$.
- At intermediate forces ($0.5 < F < 3$ pN) DNA behaves very differently if it is positively or negatively coiled. Indeed, at a force $F = F_c^- \approx 0.5$ pN, underwound DNA

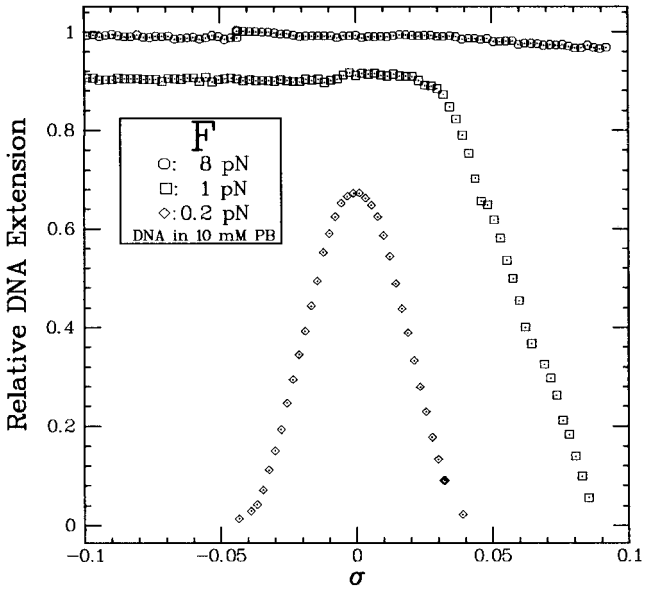

FIGURE 4 Extension versus supercoiling curves obtained for three different stretching forces in 10 mM PB. The three forces represented here were chosen to emphasize the three regimes observed in this type of experiment. In the low-force regime $F < 0.4$ pN, the DNA molecule responds in a symmetrical manner to positive or negative supercoiling by forming plectonemes. These plectonemes grow with $|\sigma|$, reducing the molecule's extension. At intermediate forces, where 0.5 pN $< F <$ 3 pN, the extension of negatively supercoiled DNA is relatively insensitive to changes in the molecule's linking number. Positively supercoiled DNA, on the other hand, contracts as the excess linking number grows. In the high force $F >$ 3 pN regime, the extensions of both positively and negatively supercoiled DNA are relatively independent of changes in the linking number.

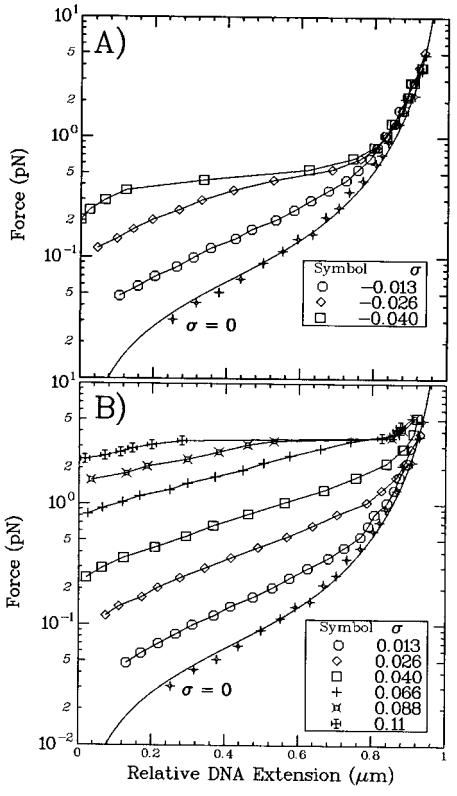

FIGURE 5 Force versus extension curves for negatively (*A*) and positively (*B*) supercoiled DNA in 10 mM PB. The $|\sigma| = 0$ curve was fitted by a WLC with a persistence length of 48 nm. The solid curves serve as guides for the eye. At low forces ($F < 0.3$ pN) the curves are similar for positive and negative supecoiling, whereas at $F_c^- \approx 0.5$ pN the negatively supercoiled molecule undergoes an abrupt transition to an extended state that behaves like a molecule with $\sigma = 0$. The positively supercoiled DNA undergoes a similar abrupt transition to an extended state when $\sigma > 0.07$ and $F = F_c^+ \approx 3$ pN.

undergoes an abrupt transition to an extension similar to that of a torsionless molecule. On the other hand, overwound DNA extends continuously as the stretching force is increased.

- At higher forces (10 pN $> F >$ 3 pN) DNA, whether under- or overwound, has a force versus extension behavior similar to that of a torsion-free DNA. There is only a weak coupling between twist and stretch. Indeed, at $F = F_c^+ \approx 3$ pN, positively coiled DNA with $\sigma > 0.1$ undergoes an abrupt transition to an extended state, in a manner similar to that observed for underwound molecules at $F_c^- \approx 0.5$ pN.

(Note: F_c^- and F_c^+ are defined as the forces needed to bring the DNA to the middle of the extension plateau.)

Supercoiled DNA in low ionic conditions (1 mM PB)

As can be seen in Fig. 6, the force-extension curves generated here for positive and negative supercoiling differ from the ones obtained in 10 mM PB. The abrupt transitions observed in the DNA's force-extension curve at 10 mM PB become more gradual in 1 mM PB. There is still a threshold force above which the supercoiled DNA behaves like a torsionally relaxed molecule, yet the transition to this behavior is no longer as abrupt. Moreover, the forces F_c^- and F_c^+ characterizing these transitions are lower than in 10 mM PB. Indeed, we observe an F_c^+ of ~1 pN, and F_c^- is now ~0.2 pN.

Supercoiled DNA in high ionic conditions (10 mM PB supplemented with 150 mM NaCl or 5 mM $MgCl_2$)

Here we introduced different cations into the system before repeating the above experiments. Except for very positive supercoiling ($\sigma \geq 0.16$), the force-extension curves and the extension versus supercoiling curves are similar to those obtained for 10 mM PB. The main difference is, once again, in the variation with the ionic conditions of the critical forces F_c^- and F_c^+.

Fig. 6 shows that the addition of 150 mM NaCl leads to a marked increase in the values for F_c^+ and F_c^-. Indeed, F_c^- increases from ~0.4 pN to ~1 pN. At the same time, F_c^+ increases from ~3 pN to 7 pN. Adding 5 mM $MgCl_2$ to the standard 10 mM PB solution leaves F_c^- unchanged at ~0.45 pN, whereas F_c^+ increases to 6.5 pN (Fig. 6).

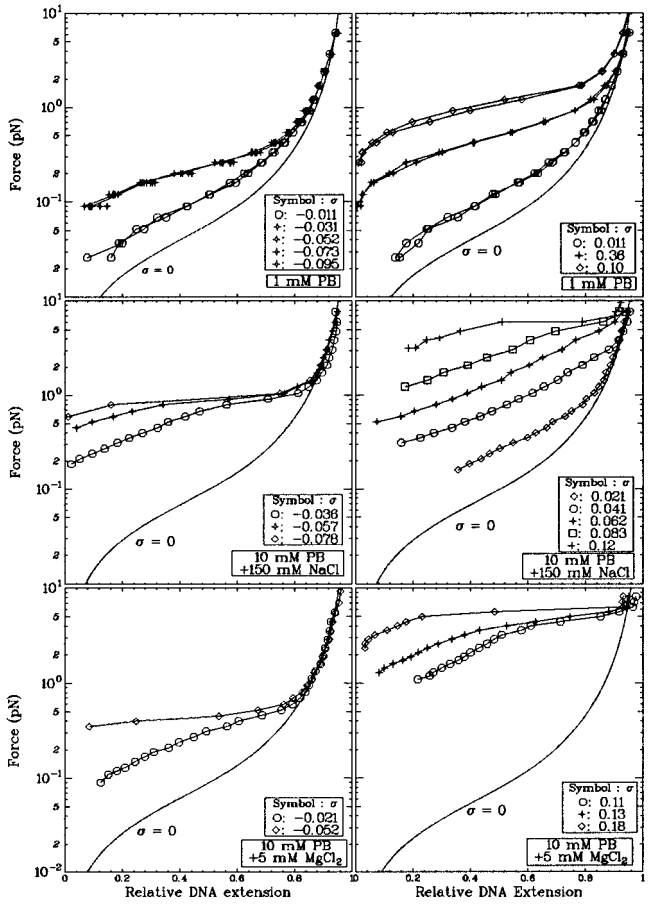

FIGURE 6 Force versus extension curves for negatively (*left column*) and positively (*right column*) supercoiled DNA in various ionic conditions. From top to bottom: 1 mM PB, 10 mM PB + 150 mM NaCl, and 10 mM PB + 5 mM $MgCl_2$. Note that these curves are qualitatively similar to those in Fig. 5. The main differences are the changes in the critical forces F_c^- and F_c^+.

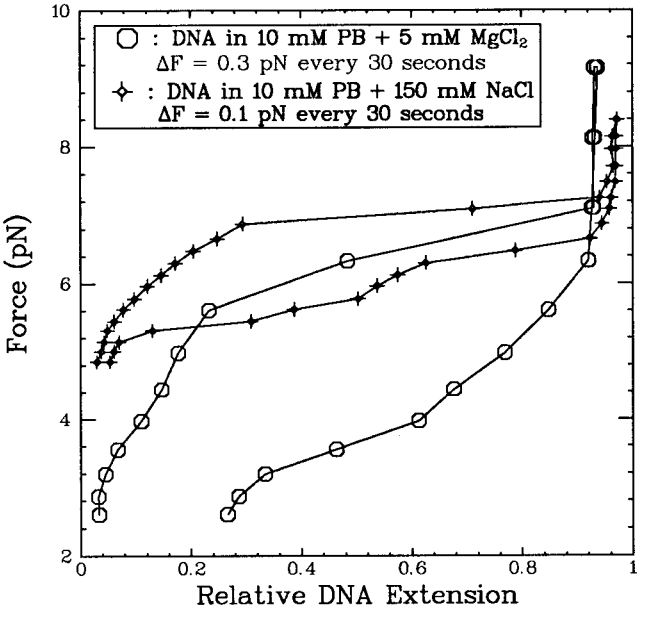

FIGURE 7 Hysteretic effect in the force versus extension curves of highly overwound ($\sigma = 0.16$) DNA in strong ionic conditions (10 mM PB + 5 mM $MgCl_2$ or 10 mM PB + 150 mM NaCl). We stretched these molecules past $F = F_c^+ \approx 7$ pN before relaxing them. Each point was taken at ~30-s intervals. For the experiment involving magnesium cations, the force changes by ~0.3 pN each step, whereas the change is ~0.1 pN for the experiment involving sodium cations. The hysteresis observed under these conditions tends to disappear as the relaxation process is made more gradual (i.e., as the time interval between successive points is increased or as the force step is decreased).

Hysteretic effect on highly supercoiled DNA in high salt conditions

In general, the extension of a coiled DNA molecule at a given force is independent of whether it was reached by stretching the molecule from a relaxed state or relaxing it from a stretched one, i.e., there is in general no observable hysteresis in the force versus extension curves of supercoiled DNA. However, this is not true for highly overwound DNA in high salt conditions ($\sigma \approx 0.16$ with 150 mM NaCl or 5 mM $MgCl_2$). Upon increasing the force past $F_c^+ \approx 7$ pN, we observe an abrupt extension of the molecule. However, if we subsequently decrease the force below F_c^+, we do not observe a concurrent abrupt shortening of the molecular extension (as for $\sigma < 0$) (Fig. 7). Instead, the molecule undergoes a continuous, history-dependent shortening as the force is decreased below F_c^+. If the force is relaxed by a ~0.3-pN step every 30 s, one can observe very significant differences between the stretching and relaxing processes. If we decrease the force interval between successive points to ~0.1-pN steps every 30 s, the relaxation curve converges toward the force versus extension curve observed while stretching.

Braided DNA in various ionic conditions

These experiments were performed by selecting magnetic beads tethered by two torsionally unconstrained λ-DNA molecules. In this case we shall consider the number of times n that the two strands of DNA are wrapped around each other when the bead is rotated in one sense or the other. Force versus extension experiments (Fig. 8) were performed in 10 mM PB by wrapping the two DNAs by $n = \pm 300$ turns before stretching. The elasticity of this type of system is seen to be independent of the sign of the wrapping. Extension versus braiding experiments (Fig. 9) were done in 1 mM PB, 10 mM PB, and 10 mM PB + 10 mM $MgCl_2$. The extension versus braiding curves were obtained at a stretching force of ~4 pN and are independent of the sign of the braiding. Two regimes were detected for the experiments concerning 1 mM PB and 10 mM PB: the first with a rapid shortening of the system for each additional turn ($n > -200$ turns in 1 mM PB and $|n| < 400$ turns in 10 mM PB), and the second with a much more gradual slope ($n < -200$ turns in 1 mM PB and $|n| > 400$ turns in 10 mM PB). The transition between the two regimes is characterized by a hysteretic behavior in the extension of the system if we

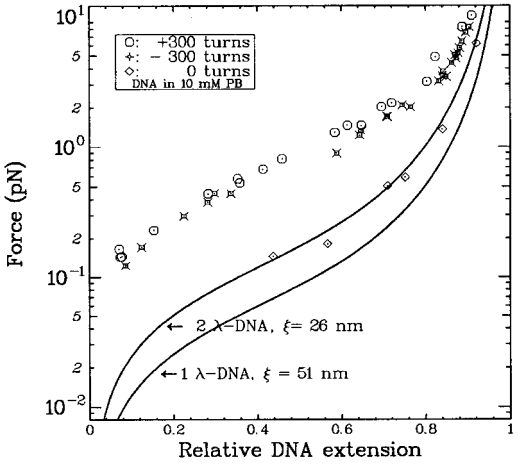

FIGURE 8 Force versus extension diagram for two nicked DNA molecules wrapped around each other 300 times in 10 mM PB. The elasticity of this system is independent of the sign of the braiding. The topmost continuous curve is the WLC prediction for stretching two unbraided molecules: $\xi \approx 26$ nm.

progressively increase rather than decrease the number of turns. The response of two DNA molecules to braiding in 10 mM PB + 10 mM $MgCl_2$ is quite different; two regimes are again apparent, but here the system responds much more vigorously to additional wrapping once a threshold number of turns ($|n| \approx 600$) is passed. No hysteretic behavior was observed in the presence of magnesium ions.

DISCUSSION

Comparison with theoretical results on stretched coiled DNA

The elastic experiments on supercoiled DNA reported here were all carried out in a regime in which the molecule is not stretched beyond l_0. In these experiments the applied force F is balanced by an entropic force, i.e., by the natural tendency of a polymer (or any molecular system) to maximize its entropy (its number of configuration, its disorder; Reif, 1965; Flory, 1969; de Gennes, 1979). The theory of stretched supercoiled DNA in this entropic regime has been developed by Marko and Siggia (1994, 1995). Here we shall just sketch their arguments and compare their predictions with our results.

The energy E for stretching a DNA molecule to a length l is (Marko and Siggia, 1995)

$$E = \frac{k_B T}{2} \int_0^{l_0} ds[\xi(\partial_s^2 \vec{r})^2 + C\Omega^2] - Fl \qquad (6)$$

where $\xi = 53$ nm and $C \approx 75$ nm (Marko and Siggia, 1995) are the persistence lengths for bending and torsion, respectively; s is the curvilinear coordinate along the molecule; $\vec{r}(s)$ is its 3D position; $|\partial_s^2 \vec{r}|$ is the local curvature; and $\Omega(s)$ is the local change in the twist rate ω_0 ($= 2\pi/h_0 = 1.85$ nm^{-1} for B-DNA with a pitch $h_0 = 3.4$ nm). The first term in the integral is the energy associated with the local bending of the molecule. The second is the torsional energy associated with a change in the local twist. The last term Fl takes care of the length constraint.

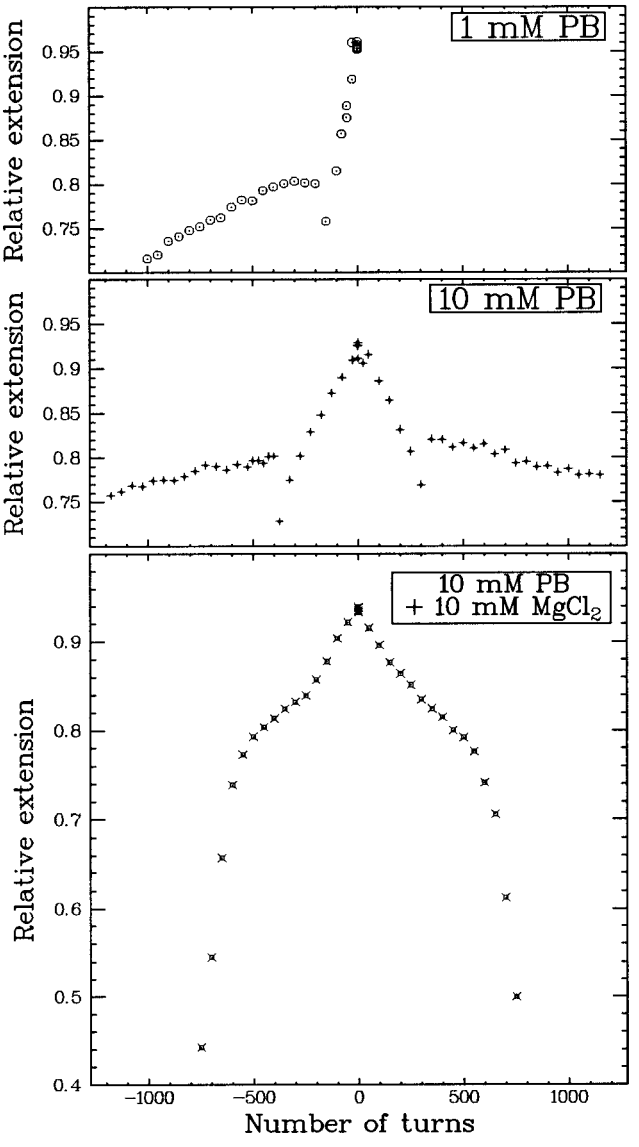

FIGURE 9 Extension versus number of turns for two DNA molecules wrapped around each other n times. Experiments were performed at a stretching force of 4 pN in 1 mM PB, 10 mM PB, and 10 mM PB supplemented with 10 mM $MgCl_2$. In the absence of magnesium cations, two regimes are apparent. In the first regime ($n > -200$ for 1 mM PB and $|n| < 400$ for 10 mM PB) the system begins by shrinking rapidly with each additional turn. The values for the effective DNA diameter as a function of ionic strength were extracted from data obtained in this regime. The second regime ($n < -200$ for 1 mM PB and $|n| > 400$ for 10 mM PB) is reached via an abrupt hysteretic transition in the system's extension and is characterized by a much weaker response to wrapping. These two regimes are not apparent in the extension versus wrapping diagram of two braided DNAs in the presence of 10 mM magnesium ions.

To actually determine the extension of a supercoiled molecule, one has to calculate its partition function (Reif,

1965), i.e., the sum over all of its possible configurations $\{\vec{r}(s), \Omega(s)\}$ of extension l and supercoiling σ weighted by their Boltzmann factor: $\exp(-E/k_BT)$. That is a tall order that has not yet been fulfilled. Instead, Marko and Siggia simplified the problem by calculating the free energy of two particular configurations. One is a plectonemic supercoil whose free energy depends only on its degree of supercoiling σ_p: $\mathcal{E}_p(\sigma_p)$. The other is a stretched solenoidal supercoil whose free energy depends on the force F and the degree of supercoiling σ_s: $\mathcal{E}_s(F, \sigma_s)$.

They went on to solve the problem of a stretched coiled DNA by assuming that its configuration can be partitioned into a portion p in plectonemic form and another $1 - p$ in stretched solenoidal form. The molecule's free energy then becomes

$$\mathcal{E} = p\mathcal{E}_p(\sigma_p) + (1 - p)\mathcal{E}_s(F, \sigma_s) \tag{7}$$

and its degree of supercoiling obeys

$$\sigma = p\sigma_p + (1 - p)\sigma_s \tag{8}$$

The minimum of the free energy $\mathcal{E}_{min}(F, \sigma)$ is calculated by minimizing $\mathcal{E}$ under p and σ_p (thus determining the fraction of plectonemes at a given force). The DNA's extension is

$$l = -\frac{\partial \mathcal{E}_{min}(F, \sigma)}{\partial F} \tag{9}$$

Because the DNA's energy (Eq. 6) is symmetrical under $\Omega \rightarrow -\Omega$, that approach predicts extensions that are identical for σ and $-\sigma$. One might thus expect its results to apply in the low-force regime. Unfortunately in this low-force, low-extension (and low σ) regime, the assumptions made by Marko and Siggia (1995) are uncontrolled. Moreover, to describe the abrupt transitions at F_c^- and F_c^+, one has to introduce further assumptions, such as the existence of alternative DNA structures (see below) for values of σ_p greater than some arbitrary thresholds.

Despite these shortcomings, the theoretical results are in good agreement with our measurements (see Marko (1997) for a comparison). This is particularly true for $0.01 < \sigma < 0.1$, in a range in which we see no abrupt transitions in the force versus extension curves and in which one expects Marko and Siggia's approach to be valid with no ad hoc assumptions on the appearance of alternative DNA structures. For $\sigma < -0.01$, fits were obtained by setting the energy barrier between the B-form of DNA and the denatured form of DNA at $\sim 2.4k_BT$ per base pair. For small degrees of supercoiling ($|\sigma| < 0.01$), however, a more detailed approach is required (Bouchiat and Mezard, 1997; J. D. Moroz and P. Nelson, manuscript in preparation).

Interpretation of F_{c^-} and F_{c^+}

Biological experiments indicate that negatively supercoiled DNA molecules alleviate excess torsional stress by denaturing locally (Palacek, 1991; Kowalski et al., 1988; Benham, 1992). These experiments hint at the fact that the alternative DNA structure that appears in stretched, unwound DNA is also a denaturation bubble. We propose that the abrupt lengthening of the underwound molecule at the critical force F_c^- is due to the simultaneous destruction of plectonemic structures and local denaturation of the DNA. At low stretching forces, an unwound DNA molecule can store its linking number deficit by writhe in plectonemic structures. As the stretching force is increased, however, the plectonemes are progressively removed and the linking number deficit must be stored by negatively twisting the double helix. As the twist of the double helix continues to become more negative, the torque acting on the two strands increases until it forces the strands to separate locally. The separated strands thus absorb the molecule's linking number deficit and allow for the remainder of the DNA to adopt a natural B-form conformation. A similar argument can be made for the transition observed at F_c^+, in which the molecule's overwinding is stored in local regions with a strong helical pitch.

$F < F_{c^-}$

When negatively supercoiled DNA is subjected to stretching forces that are lower than F_c^-, our data (Fig. 4) indicate that the DNA molecule responds to variations in the degree of supercoiling by changing its writhe Wr. Indeed, Fig. 4 indicates that there is a range of supercoiling in which the DNA's extension is linearly related to $|\sigma|$. The constant shrinking (lengthening) of the DNA molecule as a function of increasing (decreasing) $|\sigma|$ implies the regular formation (disappearance) of plectonemes as a way of relieving superhelical stress in the molecule. Thus at low force ($F < F_c^-$) and in 10 mM PB we typically measure an extension (or shortening) of ~ 0.08 μm per turn. This result is consistent with the microscopic observations of Boles et al. (1990) and Bednar et al. (1994). They measure (for $F \approx 0$) a typical plectonemic radius (Boles et al., 1990) of $r \approx 100$ Å, a pitch (Boles et al., 1990) of $p \approx 140$ Å, and a partition ratio (Bednar et al., 1994) of $Wr/Lk \approx 0.8$ (i.e., for every extra 10 turns, 8 are absorbed in plectonemes). One thus expects that every extra turn is absorbed in an increase in the plectonemic length Δl (decrease in the measured extension):

$$\Delta l \approx \sqrt{(2\pi r)^2 + p^2}\,\frac{Wr}{Lk} \approx 0.085\ \mu\text{m} \tag{10}$$

It is interesting to note that when the ionic strength of the solution was increased by adding 150 mM NaCl, the rate of shortening of the molecule decreased to ~ 0.06 μm per turn (data not shown). This is consistent with results that point to a decrease in the DNA's effective diameter (and thus a decrease in the plectonemic diameter) as the ionic strength of the solution is increased (Bednar et al., 1994).

2. $F > F_c^-$

Let us now consider the regime where $F > F_c^-$. As the force is increased the plectonemes disappear, and to satisfy White's theorem (Eq. 1) writhe is transferred into twist. As the change in twist $\Delta Tw = |Tw - Tw_0|$ is increased, the torsional stress (torque) Γ on the double helix grows as

$$\Gamma = k_B T(2\pi/h_0)C\Delta Tw/Tw_0 \qquad (11)$$

where $C \approx 75$ nm is the DNA torsional stiffness and the double helix's pitch $h_0 \approx 3.4$ nm. There is ample evidence (Palacek, 1991; Boles et al., 1990) that negatively supercoiled DNA cannot change its twist (or helical pitch) by more than ~1% to accommodate a deficit of linking number. We thus estimate that an underwound DNA is incapable of withstanding a torque $\Gamma > \Gamma_c^- \approx k_B T$. In that case, the molecule responds by denaturing locally while maintaining in the nondenatured portion a slighly subcritical twist deficit (ΔTw_c) and torsional stress, Γ_c^-.

In other words, as the twist is increased there is a point where it becomes energetically more favorable for the molecule to denature locally and partially relax its twist. This denaturation corresponds to the formation of a small bubble, along which the two constituent strands no longer wrap around each other. Effectively, the linking number of the bubble is zero ($\sigma_{bubble} = -1$), as denaturation implies a radical separation of the two strands. Thus the formation of a denaturation bubble allows for a small region of the molecule to absorb a large part of the DNA's linking number deficit. For example, a λ-DNA with a 500-bp denaturation bubble can accommodate a linking number deficit of up to 50 turns. Such a molecule, denatured over 500 bp, is nearly torsionally relaxed along the remaining 48 kb. The near-complete torsional relaxation of the remainder of the molecule after the appearance of a denaturation bubble can explain why, for forces $F > F_c^-$, the DNA behaves globally like a torsionally relaxed molecule (Marko and Siggia, 1995).

The same description also applies to positively supercoiled DNA if instead of a melted region, one assumes that the excess linking number is concentrated into regions of hypercoiled DNA, with the overwound phosphate backbone inside and the unpaired bases exposed on the outside (Pauling and Corey, 1953; R. Lavery, personnal communication; manuscript in preparation). Transient pairing between the exposed bases, especially at high salt concentration, might hinder the regular formation of plectonemes as the molecule is slowly relaxed. This could account for the observed hysteretic behavior of highly overwound DNA at high ionic strengths. Numerical simulations of positively supercoiled and stretched DNA might shed light on the possible structures of such molecules.

If we assume that local melting is the preferred response of negatively supercoiled DNA to tension greater than F_c^-, then the increase in critical forces we observe upon adding 150 mM NaCl to our experiment is consistent with results showing an increase in the melting temperature of DNA as the ionic strength is increased (Saenger, 1988). More perplexing is the fact that adding 5 mM $MgCl_2$ to the initial 10 mM PB leaves F_c^- unchanged but raises F_c^+ to that observed in 150 mM NaCl.

Energy of denaturation of DNA

In the following we shall use the force versus extension measurements on supercoiled DNA to estimate the free energy of melting. We shall assume that the denaturation bubble is completely formed once the DNA is in its extended state and shall take into account the residual twist in the nondenatured portion.

Consider first the case where DNA is coiled at low force (extension) by $n = +90$ turns to a state A^+ (Fig. 10 *A*),

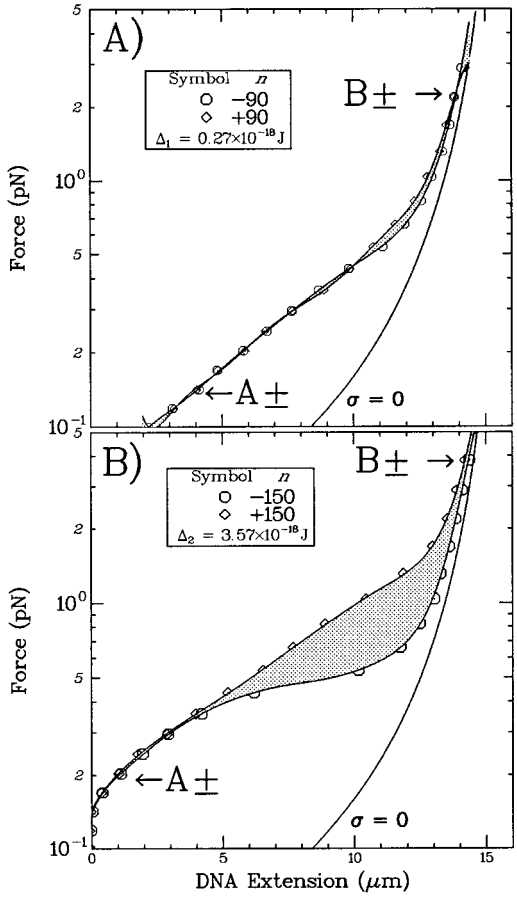

FIGURE 10 Estimating the energy of denaturation of DNA. (*A*) ○, DNA unwound by $n = -90$ turns. ◇, DNA overwound by $n = 90$ turns. The solid curves are polynomial fits to the force-extension data. The bottom curve is the theoretical (worm-like chain) fit to the data obtained for this molecule at $\sigma = 0$: $l \approx 15.7$ μm and $\xi \approx 48$ nm (Bustamante et al., 1994). The shaded surface between the σ_+ and σ_- curves represents the work Δ_1. (*B*) ○, DNA unwound by $n = -150$ turns. ◇, DNA overwound by $n = 150$ turns. The shaded surface between the σ_+ and σ_- curves represents the work Δ_2. In both cases, point A^+ (respectively, A^-) is reached by overwinding (underwinding) the DNA, which is initially at low extension (point A, not shown). Point B^+ (B^-) is reached either by stretching the molecule along the $\sigma = 0$ curve and then overwinding (underwinding) it, or by coiling the DNA to A^+ (A^-) and then stretching it via the appropriate $\sigma > 0$ ($\sigma < 0$) curve to point B^+ (B^-).

requiring a twist energy T_{A+}. The molecule is then extended (via the $\sigma = 0.02$ curve) to state B^+ so as to pull out its plectonemes. The work performed is W_{A+B+}. Alternatively, the molecule could have first been stretched (at a cost W_{AB}) and then twisted (requiring twist energy T_{B+}) by 90 turns. Therefore, $T_{A+} + W_{A+B+} = T_{B+} + W_{AB}$. Writing $W_{A+B+} - W_{AB} = \Delta W_{AB+}$,

$$T_{A^+} = T_{B^+} - \Delta W_{AB^+} \tag{12}$$

Consider now the case in which DNA is coiled by $n = -90$ turns (Fig. 10 *A*). The same reasoning as above can be applied to the negatively coiled states A^- and B^- to $T_{A-} + W_{A-B-} = T_{B-} + W_{AB}$, and thus

$$T_{A^-} = T_{B^-} - \Delta W_{AB^-} \tag{13}$$

When one unwinds the prestretched molecule at a cost of T_{B-}, however, part of that energy (E_c, obtained by twisting the DNA n_c times) goes into the molecule's twist, and the remainder (E_{d1}) goes toward denaturing the DNA over $10.4 \times n_{d1}$ bp. Therefore, $T_{B-} = E_c + E_{d1}$, and

$$T_{A^-} = E_c + E_{d1} - \Delta W_{AB^-} \tag{14}$$

In the low extension state A^-, the molecule has torsional energy $T_{A-} = T_{A+}$, because at low force the molecule behaves similarly under positive or negative coiling (Strick et al., 1996). Hence

$$T_{B^+} - \Delta W_{AB^+} = E_{d1} + E_c - \Delta W_{AB^-} \tag{15}$$

so that $E_{d1} + E_c = T_{B+} - \Delta_1$ (with $\Delta_1 = \Delta W_{AB+} - \Delta W_{AB-}$). T_{B+} is simply the energy of a rod with torsion constant C twisted by n_1 turns:

$$E_{d1} + \frac{k_B T}{2}\frac{C}{l_0}(2\pi n_c)^2 = \frac{k_B T}{2}\frac{C}{l_0}(2\pi n_1)^2 - \Delta_1 \tag{16}$$

where $n_1 = n_{d1} + n_c$, $E_{d1} = 10.4 \times n_{d1} \times E_{denaturation/basepair}$, k_B is the Boltzmann constant, T is the temperature, and C is the DNA's torsional stiffness.

Because E_c is independent of the molecule's degree of unwinding, it can be eliminated by subtraction from Eq. 16 if we perform the same experiments at a different $|\sigma|$. Using, for example, $n_2 = \pm 150$ turns (Fig. 10 *B*), we can write the same type of equation as above (using again points A and B to denote the low- and high-extension states):

$$E_{d2} + E_c = T_{B^+} - \Delta_2 \tag{17}$$

where E_{d2} is the energy of denaturation for $n_2 = n_{d2} + n_c$ turns and Δ_2 is effectively the surface between curves A^+B^+ and A^-B^- obtained for $|\sigma| = 0.033$. Subtracting the two equations yields

$$E_{d2} - E_{d1} = 2\pi^2 k_B T \frac{C}{l_0}(n_2^2 - n_1^2) - [\Delta_2 - \Delta_1] \tag{18}$$

The difference $E_{d2} - E_{d1}$ corresponds to the energy involved in converting $n_2 - n_1$ supercoils into a denaturation bubble. We take $k_B T = 4.1 \times 10^{-21}$ J, $l_0 = 15.8$ μm $\pm$ 3%, and evaluate $\Delta_1 = 0.27 \times 10^{-18}$ J for $n_1 = 90$ turns and $\Delta_2 = 3.57 \times 10^{-18}$ J for $n_2 = 150$ turns. These energies are evaluated to within 10%. There is no error in the numbers n_1 and n_2, yet there is an uncertainty of two to three turns in the determination of the rotational zero ($\sigma = 0$) of the molecule. Because the value of C is not very well known, we write

$$E_{denaturation/bp}(k_B T) = 0.029 k_B T/\text{nm} \times C - 1.3 k_B T \tag{19}$$

Table 1 shows how the enegy of denaturation per base pair varies with C. It is interesting to note that a value of C lower than 45 nm would lead to a negative energy of denaturation and can thus be excluded.

We can compare this estimate with the expected energy of denaturation per base pair in A-T-rich regions $\Delta G_{25°}$ (at $T = 25$°C and in a ~20 mM NaCl solution). Using a typical heat of helix formation $\Delta H = -8$ kcal/mol (per bp) (Bloomfield et al., 1974) and a typical melting temperature for poly(dA)poly(dT) DNA (Saenger, 1988), $T_m = 53$°C (in 20 mM NaCl), we obtain (Bloomfield et al., 1974) $\Delta G_{25°} = \Delta H\,(1 - T/T_m) = 0.68$ kcal/mol $\approx 1.1\ k_B T$. Because the energy of denaturation (at 25°C) of GC-rich regions is 0.75 kcal/mol bp ($\sim 1.25 k_B T$) higher than that of AT-rich regions (Bloomfield et al., 1974), we conclude that the denaturation bubble is localized in AT-rich regions.

Behavior of two braided DNA molecules

As pointed out earlier, the force-extension and extension-coiling diagrams obtained for the braiding of two DNA molecules (Marko, 1997) indicate that the system behaves identically under positive or negative wrapping (Figs. 8 and 9). If we consider each DNA to be a tube of diameter D and extension l_0, a simple model allows us to estimate the effective diameter of a DNA molecule. When the molecules are wrapped around each other n times, the effective length l of the system decreases:

$$l = \sqrt{l_0^2 - (\pi D n)^2} \tag{20}$$

This is the simplest possible model, and it assumes that the stretching force applied to the system is sufficiently high to prevent the extrusion of plectonemic-like structures. Fitting this equation to the $n < 300$ turns regime in our experimental data on the braiding of two molecules (Fig. 9) yields $D \approx 7.5 \pm 1$ nm for DNA in a 10 mM phosphate

TABLE 1 The energy of denaturation per base pair (in $k_B T$) as a function of the DNA torsion constant C

C (nm)	$E_{denat/bp}$ ($k_B T$)
50	0.15
60	0.44
70	0.73
80	1
90	1.3
100	1.6

buffer, consistent with previous measurements (Bednar et al., 1994). The curvature in this regime becomes stronger when the ionic conditions are lowered to 1 mM PB, indicating that the effective diameter of the DNA increases to ~20 nm. Adding 10 mM $MgCl_2$ to the 10 mM PB solution, however, reduces the curvature slightly, giving an effective diameter on the order of 5 nm. These trends are consistent with what is known about the salt dependence of a DNA's effective diameter. As one increases the concentration of cations, the electrostatic repulsion between two strands of DNA decreases as the negative charge of the molecule is progressively screened. At low ionic strengths, this repulsion is greater and results in an increase in the molecule's effective diameter. Unfortunately, the DNA construction we use does not allow us to anchor the two molecules to the same points at the surface and on the magnetic bead. Thus the precise geometry of the system cannot be determined and may influence the response to wrapping.

We also observe very curious transitions in the extension versus effective coiling of two DNA molecules above a certain number of turns. These transitions, observed in 1 and 10 mM PB, are hysteretic and point to the presence of a first-order transition in the structure of two braided molecules. These transitions may be associated with the fact that the electrostatic potential between two charged molecules is not a hard-core potential, but can be overcome by the energy added to the system as it is braided (e.g., forced) together (Timsit and Moras, 1995). The facts that 1) the onset of the transition depends on the ionic conditions and 2) the transition disappears when 10 mM $MgCl_2$ is added to the experiment hint at an electrostatic origin for this transition. These experiments show that the behavior of two braided DNA molecules is very rich in surprises—including a possible electrostatic collapse of the system—but that a more controllable form of the construction must be designed before we are able to achieve more quantitative results.

CONCLUSION

The stretching of over- and underwound single DNA molecules in various salt conditions reveals the existence of three regimes:

- A low-force regime ($F < F_c^-$) in which over- and underwound molecules behave similarly under stretching. Here they transfer the excess or deficit of their linking number into positive or negative writhe, thereby increasing the portion of plectonemic supercoils.
- An intermediate force regime ($F_c^- < F < F_c^+$) in which underwound molecules locally denature to relax the torsional stress due to the increased twist. On the other hand, overwound DNA resists the increased twist resulting from the disappearance of plectonemes and decrease in writhe.
- A high-force regime ($F > F_c^+$) in which supercoiled DNA behaves quite like a torsionless molecule. In particular, sufficiently overwound molecules ($\sigma > 0.1$) yield (at $F = F_c^+$) to the increased torsional stress resulting from the decrease in writhe. That transition, similar to the one occurring (at $F = F_c^-$) in underwound molecules, implies the formation of local regions of highly overwound DNA. The detailed structure of DNA in these regions remains a puzzle, which could be related to the observed hysteretic behavior of stretched overwound DNA in high salt.

As expected and in contrast with the behavior of a single torsionally constrained molecule, the stretching of two braided nicked DNA molecules is symmetrical under $\sigma \rightarrow -\sigma$. The wealth of quantitative information gathered in these experiments (persistence length, DNA length and diameter, rate of plectoneme formation, energy of denaturation) demonstrate the usefulness of the single molecule manipulation technique used here.

We especially thank Catherine Schurra for the preparation of silanized capillaries and the late François Caron for letting us use his pXΔ1 supercoilable construct. We also thank Aaron Bensimon, Steve Block, Claude Bouchiat, Carlos Bustamante, Richard Lavery, John Marko, Marc Mézard, Philip Nelson, Olivier Hyrien, Eric Siggia, Steve Smith, and Youri Timsit for fruitful discussions.

We acknowledge the support of the CNRS, Universités Paris 6 and Paris 7, and the Ecole Normale Supérieure. T.R.S. was supported by a CNRS doctoral fellowship.

REFERENCES

Allemand, J. F., D. Bensimon, L. Jullien, A. Bensimon, and V. Croquette. 1997. pH-Dependent specific binding and combing of DNA. *Biophys. J.* 73:2064–2070.

Beattie, K. L., R. C. Wiegand, and C. M. Radding. 1977. Uptake of homologous single-stranded fragments by superhelical DNA. *J. Mol. Biol.* 116:783–803.

Bednar, J., P. Furrer, A. Stasiak, and J. Dubochet. 1994. The twist, writhe and overall shape of supercoiled DNA change during counterion-induced transition from a loosely to a tightly interwound superhelix. *J. Mol. Biol.* 235:825–847.

Benham, C. J. 1992. Energetics of the strand separation transition in superhelical DNA. *J. Mol. Biol.* 225:835–847.

Bensimon, A., A. J. Simon, A. Chiffaudel, V. Croquette, F. Heslot, and D. Bensimon. 1994. Alignment and sensitive detection of DNA by a moving interface. *Science.* 265:2096–2098.

Bloomfield, V. A., D. M. Crothers, and I. Tinoco, Jr. 1974. Physical Chemistry of Nucleic Acids. Harper and Row, New York.

Boles, T. C., J. H. White, and N. R. Cozzarelli. 1990. Structure of plectonemically supercoiled DNA. *J. Mol. Biol.* 213:931–951.

Bouchiat, C., and M. Mezard. 1998. Elasticity model of a supercoiled DNA molecule. *Phys. Rev. Lett.* (in press).

Bustamante, C., J. F. Marko, E. D. Siggia, and S. Smith. 1994. Entropic elasticity of λ-phage DNA. *Science.* 265:1599–1600.

Calladine, C. R., and H. R. Drew. 1992. Understanding DNA. Academic Press, San Diego.

Cluzel, P. 1996. L'ADN, une molécule extensible. Ph.D. thesis. Université Pierre et Marie Curie, Paris.

Cluzel, P., A. Lebrun, C. Heller, R. Lavery, J.-L. Viovy, D. Chatenay, and F. Caron. 1996. DNA: an extensible molecule. *Science.* 271:792–794.

de Gennes, P.-G. 1979. Scaling Concepts in Polymer Physics. Cornell University Press, Ithaca, NY.

Dunaway, M., and E. A. Ostrander. 1993. Local domains of supercoiling activate a eukaryotic promoter in vivo. *Nature.* 361:746–748.

Flory, P. J. 1969. Statistical Mechanics of Chain Molecules. Wiley Interscience, New York.

Gelles, J., B. J. Schnapp, and M. Sheetz. 1988. Tracking kinesin-driven movements with nanometre-scale precision. *Nature.* 331:450–453.

Jannink, G., B. Duplantier, and J.-L. Sikorav. 1996. Forces on chromosomal DNA during anaphase. *Biophys. J.* 71:451–465.

Klenin, K. V., M. D. Frank-Kamenetskii, and J. Langowski. 1995. Modulation of intramolecular interactions in superhelical DNA by curved sequences: a Monte Carlo simulation study. *Biophys. J.* 68:81–88.

Kowalski, D., D. Natale, and M. Eddy. 1988. Stable DNA unwinding, not breathing, accounts for single-strand specific nuclease hypersensitivity of specific A+T-rich sequences. *Proc. Natl. Acad. Sci. USA*. 85: 9464–9468.

Marko, J. F. 1997. Supercoiled and braided DNA under tension. *Phys. Rev. E.* 55:1758–1772.

Marko, J. F., and E. D. Siggia. 1994. Fluctuations and supercoiling of DNA. *Science.* 265:506–508.

Marko, J. F., and E. D. Siggia. 1995. Statistical mechanics of supercoiled DNA. *Phys. Rev. E.* 52:2912–2938.

Palacek, E. 1991. Local supercoil-stabilized structures. *Crit. Rev. Biochem. Mol. Biol.* 26:151–226.

Patterton, H.-G., and C. von Holt. 1993. Negative supercoiling and nucleosome cores. (I) The effect of negative supercoiling on the efficiency of nucleosome core formation in vitro. *J. Mol. Biol.* 229:623–636.

Pauling, L., and R. B. Corey. 1953. A proposed structure for the nucleic acids. *Proc. Natl. Acad. Sci. USA*. 39:84–97.

Reif, F. 1965. Fundamentals of Statistical and Thermal Physics. McGraw-Hill, New York.

Saenger, W. 1988. Principles of Nucleic Acid Structure. Springer Verlag, New York.

Schlick, T., and W. K. Olson. 1992. Supercoiled DNA energetics and dynamics by computer simulation. *J. Mol. Biol.* 223:1089–1119.

Smith, S. B., Y. Cui, and C. Bustamante. 1996. Overstretching B-DNA: the elastic response of individual double-stranded and single-stranded DNA molecules. *Science.* 271:795–799.

Smith, S. B., L. Finzi, and C. Bustamante. 1992. Direct mechanical measurements of the elasticity of single DNA molecules by using magnetic beads. *Science.* 258:1122–1126.

Strick, T. R., J.-F. Allemand, D. Bensimon, A. Bensimon, and V. Croquette. 1996. The elasticity of a single supercoiled DNA molecule. *Science.* 271:1835–1837.

Timsit, T., and D. Moras. 1995. Self-fitting and self-modifying properties of the B-DNA molecule. *J. Mol. Biol.* 251:629–647.

Vinograd, J., J. Lebowitz, R. Radloff, R. Watson, and P. Laipis. 1965. The twisted circular form of polyoma virus DNA. *Proc. Natl. Acad. Sci. USA.* 53:1104–1111.

Vologodskii, A. V., S. D. Levene, K. V. Klenin, M. D. Frank-Kamenetskii, and N. R. Cozzarelli. 1992. Conformational and thermodynamic properties of supercoiled DNA. *J. Mol. Biol.* 227:1224–1243.

Wang, J. C. 1996. DNA topoisomerases. *Annu. Rev. Biochem.* 65: 635–692.

Wang, Z., and P. Dröge. 1997. Long-range effects in a supercoiled DNA domain generated by transcription in vitro. *J. Mol. Biol.* 271:499–510.

White, J. H. 1969. Self-linking and the gauss integral in higher dimensions. *Am. J. Math.* 91:693–728.

Wu, H.-Y., S. Shyy, J. C. Wang, and L. F. Liu. 1988. Transcription generates positively and negatively supercoiled domains in the template. *Cell.* 53:433–440.